

Winter 12-7-2009

# Viscosity Dependent Liquid Slip at Molecularly Smooth Hydrophobic Surfaces

Sean P. McBride

Marshall University, [mcbrides@marshall.edu](mailto:mcbrides@marshall.edu)

Bruce M. Law

Follow this and additional works at: [http://mds.marshall.edu/physics\\_faculty](http://mds.marshall.edu/physics_faculty)



Part of the [Physics Commons](#)

---

## Recommended Citation

McBride, S. P., & Law, B. M. (2009). Viscosity-dependent liquid slip at molecularly smooth hydrophobic surfaces. *Physical Review E*, 80(6), 060601.

This Article is brought to you for free and open access by the Physics at Marshall Digital Scholar. It has been accepted for inclusion in Physics Faculty Research by an authorized administrator of Marshall Digital Scholar. For more information, please contact [zhangj@marshall.edu](mailto:zhangj@marshall.edu), [martj@marshall.edu](mailto:martj@marshall.edu).

## Viscosity-dependent liquid slip at molecularly smooth hydrophobic surfaces

Sean P. McBride and Bruce M. Law

*Department of Physics, Cardwell Hall, Kansas State University, Manhattan, Kansas 66506-2601, USA*

(Received 9 March 2009; revised manuscript received 11 September 2009; published 7 December 2009)

Colloidal probe atomic force microscopy is used to study the slip behavior of 18 Newtonian liquids from two homologous series, the  $n$ -alkanes and  $n$ -alcohols, at molecularly smooth hydrophobic  $n$ -hexadecyltrichlorosilane coated surfaces. We find that the slip behavior is governed by the bulk viscosity  $\eta$  of the liquid, specifically, the slip length  $b \sim \eta^x$  with  $x \sim 0.33$ . Additionally, the slip length was found to be shear rate independent, validating the use of Vinogradova slip theory in this work.

DOI: [10.1103/PhysRevE.80.060601](https://doi.org/10.1103/PhysRevE.80.060601)

PACS number(s): 83.50.Rp, 68.37.Ps

When discussing fluid flow over a solid object, it is customary to apply the Navier-Stokes equations, assuming no-slip boundary conditions (BCs), such that the fluid velocity relative to the solid is zero at the solid-liquid interface [1]. This no-slip BC has successfully described macroscopic experiments for many years. However, recent experiments on confined liquids have demonstrated that partial slip frequently occurs at the solid-liquid interface, leading to a non-zero fluid velocity adjacent to the solid surface. Slip behavior is described by the slip length  $b$ , which is defined as the extrapolation distance into the solid surface, where the fluid velocity would be equal to zero. The study of slip BCs has become a subject of increasing importance with the advent of microfluidic and nanofluidic devices [2]. Experimental slip lengths from nanometers to microns have been reported in the literature [1]. Unfortunately, reliable measurements of the slip length have proven to be difficult to obtain [3,4]. As such, there are ongoing discussions not only as to what physical phenomena cause slip but also which of the numerous experiments constitute reliable slip measurements.

Direct evidence for slip has been determined by measuring the motion of fluorescent nanometer-sized tracer particles in solution near a solid surface [5]; however, this technique has a limited slip length resolution of  $\sim 10$  nm. Colloidal probe atomic force microscopy (AFM) and the surface forces apparatus (SFA) can provide a better slip length resolution of  $\sim 1$  nm, but care must be taken to eliminate artifacts that may mask slip behavior [3,4]. In colloidal probe AFM [6], the AFM cantilever is driven at a constant speed  $v_d$  toward the solid surface. The colloidal sphere at the end of the AFM cantilever approaches at a slower speed  $v$ , which depends upon how rapidly the liquid can be squeezed out from between the two surfaces. This changing velocity is dependent upon the solid/liquid BCs through the slip length  $b$ . The hydrodynamic force experienced by the colloidal sphere is given by

$$F_h = \frac{6\pi\eta r^2 v \psi}{h}, \quad (1)$$

where  $\eta$  is the bulk viscosity,  $r$  is the radius of the colloidal probe,  $h$  is the separation distance between the colloidal probe and the solid surface, and  $v = dh/dt$  is the measured approach velocity of the colloidal probe. For the no-slip BC, the parameter  $\psi = 1$ . From continuum hydrodynamics, Vinogradova [7] determined a relationship between  $\psi$  and the slip length  $b$  (V-theory), which is valid for  $h \ll r$ , assuming a constant slip length  $b$  independent of shear rate. For hydrophobic surfaces,

gradova [7] determined a relationship between  $\psi$  and the slip length  $b$  (V-theory), which is valid for  $h \ll r$ , assuming a constant slip length  $b$  independent of shear rate. For hydrophobic surfaces,

$$\psi = \frac{h}{3b} \left[ \left( 1 + \frac{h}{6b} \right) \ln \left( 1 + \frac{6b}{h} \right) - 1 \right]. \quad (2)$$

The experimental hydrodynamic force is measured from the bending of the AFM cantilever via Hooke's law  $F_e = kx$ , where  $k$  is the cantilever spring constant. As illustrated by Cottin-Bizonne *et al.* [8], Eqs. (1) and (2) can be expanded in the limit of large separations  $X = 6b/h \ll 1$

$$\frac{6\pi\eta r^2 v}{F_h} = h + 2b. \quad (3)$$

The key feature of this expansion is that the extrapolated experimental data should intercept the  $h$  axis at  $h = -2b$  in the absence of any experimental artifacts.

Theory [9,10] and recent experiments [3,4] indicate that for experimentally accessible shear rates ( $\dot{\gamma} \sim 10^2 - 10^5$  s $^{-1}$ ), the slip length should be constant and independent of shear rate, as assumed in the V-theory; the slip length is expected to only become shear rate dependent [9] at very high shear rates near the critical shear rate  $\dot{\gamma}_c \approx 10^{11}$  s $^{-1}$  [11] (accessible in computer simulations). Experimental measurements [12,13], which exhibit shear rate-dependent slip may indicate the presence of either nanobubbles [14,15] or nanoparticles [16] on the surface or may be a result of an incorrect determination of the zero of separation ( $h=0$ ) [4].

In this work, we use colloidal probe AFM [6] to determine the slip length against a molecularly smooth Si wafer for 18 different liquids from two homologous series; nine  $n$ -alkanes and nine  $n$ -alcohols. An advantage of this study is that the same colloidal probe and Si surface are used for all liquids. As such, relative changes in slip can be readily compared between liquids and any slip length trends can be attributed to liquid properties (because the solid surfaces remain unchanged).

In order to study low viscosity liquids, we use large silica colloidal spheres with diameters  $2r \sim 55$   $\mu\text{m}$  from Mo-Sci. Such large colloidal spheres possess additional advantages: the viscous drag on the cantilever itself [17] is negligible ( $< 1\%$ ) compared with the hydrodynamic force and larger separations  $h(\text{max}) = 2$   $\mu\text{m}$  can be used while still remaining

in the regime  $h \ll r$  required by Eq. (2). The spheres were UV glued to triangular AFM cantilevers (Veeco NP-S series) with spring constants in the range  $k \sim 0.6\text{--}1.3$  N/m. Both the Si wafer from Silicon Materials Inc. (which possessed a  $\sim 2$ -nm-thick amorphous native oxide layer) and attached silica colloidal particle were silanated with a *n*-hexadecyltrichlorosilane (Fluka) self-assembled monolayer (SAM) using a cold deposition ( $10^\circ\text{C}$ ) wet chemistry coating procedure [18] performed in a dry box. After coating, the Si wafer and silica sphere had rms surface roughnesses of 0.3 nm and less than 1 nm, respectively, as measured over a  $1\ \mu\text{m}^2$  area using tapping mode AFM. The Si surface had a uniform hydrophobic silane coating, as indicated by a water contact angle of  $107 \pm 0.7^\circ$ , *n*-dodecane contact angle hysteresis of less than  $4^\circ$ , and a critical surface tension of  $20.3 \pm 0.02$  mN/m determined from the *n*-alkane homologous series [18]. The *n*-alkanes (from *n*-heptane to *n*-hexadecane, excluding *n*-undecane) and *n*-alcohols (from *n*-ethanol to *n*-decanol), a total of 18 liquids, had a stated purity of 99+% and were used as received from Sigma Aldrich. In order to minimize adsorption of any atmospheric contaminants onto either the colloidal probe or Si wafer substrate, an atmospheric chamber was built between the Asylum 3D MFP head and base. This allows an *in situ* purging of both surfaces with 99.999+% purity  $\text{N}_2$  gas for 1 min. With the nitrogen gas turned off, the liquid to be studied was then immediately filled *in situ* under this inert gas atmosphere. After each experiment, the AFM colloidal probe/holder and Si wafer were rinsed well and/or sonicated in chloroform, blown dry with  $\text{N}_2$  gas, and then vacuum dried before the next liquid was studied. The same Si wafer was used in all experiments; each homologous series was studied with two different colloidal probes to test reproducibility.

The spring constant  $k$  is determined *in situ* using our most viscous liquid (*n*-decanol), which has the largest hydrodynamic response and therefore provides the most accurate determination of  $k$ . More specifically,  $k$  is determined from the hydrodynamic bending of the cantilever at large separations ( $h \sim 1\text{--}2\ \mu\text{m}$ ) [19] for *n*-decanol, assuming no-slip BCs ( $b=0$ ). For our system with small slip lengths  $b \sim 10\text{--}30$  nm, a no-slip BC ( $b=0$ ) is an excellent approximation at large  $h$ . With  $k$  then fixed, the slip length  $b$ , which primarily plays a role at small separations, can be determined for any liquid by comparing the experimental hydrodynamic force  $F_e \equiv F_e(h)$  with theory [ $F_h$ , Eqs. (1) and (2)] over an extended separation range ( $50\ \text{nm} < h < 2\ \mu\text{m}$ ). A slow approach ( $300\text{--}500$  nm/s) was performed prior to each hydrodynamic measurement to calibrate the voltage response of the AFM photodetector and to ensure that no nanobubbles or anomalous charges were present; only a weak van der Waals interaction was observed immediately before hard contact between the two solid surfaces.

Figure 1(a) demonstrates the excellent agreement between experimental data (circles) and V-theory with  $b=23.4$  nm (solid line) for *n*-heptanol at a cantilever drive speed  $v_d = 40\ \mu\text{m/s}$ . The theory is slightly noisy because experimental values for the speed  $v$  are used in Eq. (1). As the colloidal probe approaches the solid surface, the hydrodynamic force  $F_h$  increases from 1.5 to 40 nN as the separation  $h$  decreases from  $2\ \mu\text{m}$  to 50 nm. The effective shear rate  $\dot{\gamma}_e = v/h$  [Fig.

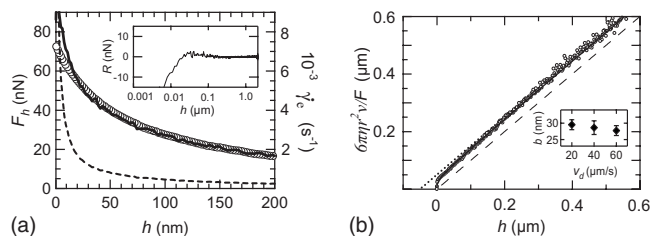


FIG. 1. (a) Hydrodynamic force  $F_h$  versus separation  $h$  for *n*-heptanol at  $v_d = 40\ \mu\text{m/s}$ ; experiment (circles), V-theory for  $b = 23.4$  nm (solid line), and effective shear rate  $\dot{\gamma}_e$  (dashed line). Inset: hydrodynamic force residuals  $R = F_e - F_h$  for *n*-heptanol. (b) Expansion representation [Eq. (3)] of *n*-heptanol data from (a); experiment (circles), V-theory for  $b = 23.4$  nm (thin solid line), experimental no-slip BC (dashed line), and extrapolation of experimental data for  $h \gg b$  (dotted line). Inset:  $b$  as a function of  $v_d$  for *n*-heptanol.

1(a), dashed line] increases from  $20\ \text{s}^{-1}$  at  $h = 2\ \mu\text{m}$  to  $1000\ \text{s}^{-1}$  at  $h = 50$  nm. The absence of systematic deviations in the residuals  $R = F_e - F_h$  [Fig. 1(a) inset] for separations  $50\ \text{nm} < h < 2\ \mu\text{m}$  implies that V-theory is in good agreement with our experimental data for constant  $b$  for this separation range. Deviations at small separations ( $h < 25$  nm) may be due to either a decreasing viscosity (shear thinning) or increasing slip length with decreasing separation; however, further work is required to ascertain the cause for these deviations. Our excellent agreement with V-theory as well as the fact that the slip length  $b$  is independent of  $v_d$  to within experimental error [Fig. 1(b), inset] provides evidence that  $b$  is shear rate independent (at least for  $h > 50$  nm).

Figure 1(b) replots the data in Fig. 1(a), using the representation in Eq. (3). The slope of the dotted line is  $1.005 \pm 0.005$ , which implies that  $\eta$  and  $r$  are accurately determined. As determined from the intercept, the slip length is  $b = 25.1$  nm, which agrees well with the value of  $b = 23.4$  nm determined in Fig. 1(a). The viscosity  $\eta$  was determined for the actual experimental temperature using [20]. Our preference is to use Eqs. (1) and (2) to determine  $b$ , as Eq. (3) is more susceptible to errors originating from extrapolating data over large distances. In the remainder of this publication, we discuss the slip length results obtained for the *n*-alkanes and *n*-alcohols at large separations ( $h > 50$  nm) where V-theory provides an excellent description of experimental data.

Both theory and computer simulations have suggested a number of causes for slip on molecularly smooth solid surfaces. If one cause dominates the others, then it should show up as a correlation in the experimental data. Three potential slip mechanisms are discussed below.

(i) If the commensurability/incommensurability of the liquid for the solid surface structure [21,22] principally determined the slip behavior, this would imply that similarly sized molecules (e.g., *n*-octane and *n*-octanol) should exhibit similar slip lengths. Figure 2 indicates that these two liquids do not exhibit similar slip lengths.

(ii) Theory suggests that the slip length  $b$  should monotonically increase with increasing contact angle  $\theta$  [23,24]. In our work, no correlation is found between the *n*-alkane and

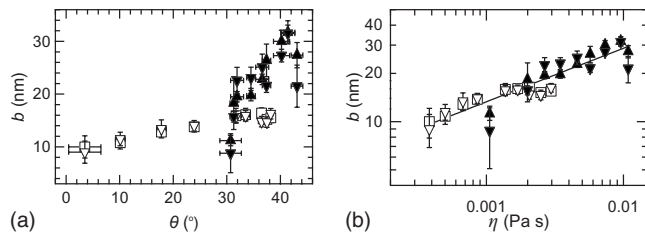


FIG. 2. (a) Slip length  $b$  versus contact angle  $\theta$  for the  $n$ -alkanes (open symbols) and  $n$ -alcohols (solid symbols). (b) Slip length  $b$  versus bulk viscosity  $\eta$  on a log-log plot for the  $n$ -alkanes (open symbols) and  $n$ -alcohols (solid symbols). The solid line is a fit to the data, as described in the text. Spring constants for the three AFM cantilevers: inverted triangles (open and solid),  $k = 1.26$  N/m; triangles,  $k = 1.31$  N/m; squares,  $k = 0.63$  N/m.

$n$ -alcohol slip length data sets when plotted as a function of contact angle [Fig. 2(a)]. Hence, the slip length is not predominantly determined by the wettability of the liquid for the solid substrate for these liquids. The slip length  $b$  error bars in Fig. 2 represent either the experimental uncertainty from a minimum of six experiments or an uncertainty of 1 nm, originating from our estimated zero in separation error [25], which ever is larger.

(iii) Theory suggests that  $b$  should increase linearly with viscosity  $\eta$  for homologous series of liquids against a structureless atomically smooth solid surface [9,10,26]. In contrast to this prediction, we find an excellent correlation between data sets [Fig. 2(b)] for  $b = A\eta^x$  with amplitude  $A = 130 \pm 60$  nm/(Pa s) $^x$  and exponent  $x = 0.33 \pm 0.17$ . An element that is missing from most theories and computer simulations is the influence of the  $n$ -alkylsilane brush on the slip behavior. The presence of this brush on both the Si surface and colloidal probe will alter how momentum is transferred from the liquid to the solid, which in turn will influence the slip behavior [10].

Theory suggests that similar slip behavior should be observed for both polymeric and nonpolymeric liquids [9]. Fetzer *et al.* [27] observed very large shear independent slip lengths while studying the dewetting dynamics of polystyrene films on  $n$ -alkylsilane-coated Si wafers. In their study, short polymer chain lengths were used, below the entanglement length [28]; hence, these polymers are expected to behave like simple Newtonian liquids in these dewetting studies. Our measurements are qualitatively consistent with the very large shear-independent slip lengths observed by Fetzer *et al.* The viscosities ( $\eta \sim 10^4 - 10^7$  Pa s) and slip lengths ( $b \sim 100 - 10\,000$  nm) were many orders of magnitude larger than the corresponding quantities studied here. For an  $n$ -dodecyltrichlorosilane (C12) coating, they found  $b \sim \eta^x$  with  $x \sim 0.5$ ; for an  $n$ -octadecyltrichlorosilane (C18) coating, the exponent showed almost zero slope ( $x \sim 0$ ) at small viscosities, which increased to a larger slope ( $x \sim 0.33$ ) at large viscosities. Our measured exponent  $x \sim 0.33$  for a  $n$ -hexadecyltrichlorosilane (C16) coating is approximately consistent with their polymer results; however, the amplitude  $A$  observed here is a factor of  $\sim 10$  larger than in the polymer experiments.

Cottin-Bizonne *et al.* [3] and Honig and Ducker [4] recently reported shear-independent slip lengths. The experimental results in [3,4] and those reported here are inconsistent with each other. The shear rate independence of  $b$  and the agreement with V-theory are indicative that each of these experiments provides a valid measure of the slip. We postulate that the differences in the slip behavior could be due to differences either in the sample surfaces or sample environment.

Honig and Ducker [4] used a colloidal probe AFM incorporating a novel evanescent wave detector to determine the zero of separation. They study slip in sucrose solutions and polydisperse polydimethylsiloxane against various hydrophilic ( $\theta < 5^\circ, 20^\circ$ ) and hydrophobic ( $\theta \sim 40^\circ, 90^\circ$ ) surfaces [29]. In all cases, their results were described by a no-slip BC ( $b = 0$ ). For binary liquid mixtures and polydisperse systems, preferential adsorption may alter the slip behavior. Honig and Ducker report a relatively large contact angle hysteresis of  $\Delta\theta \sim 15^\circ - 20^\circ$  [29]. Contact angle hysteresis is generally associated with physical or chemical roughness [30]; hence, their surfaces may be more chemically heterogeneous than our surfaces. These differences might explain their no-slip observations.

Cottin-Bizonne *et al.* used an accurate custom-designed dynamic SFA to determine slip behavior [3,8]. They examined water-glycerol mixtures against Pyrex and octadecyltrichlorosilane(OTS)-coated Pyrex [8]. They do not find the systematic variation with viscosity that we report here; preferential adsorption effects in the binary mixture may be responsible for these differences. For dodecane and water against various solid surfaces, they reported a strong divergence in the slip length for  $\theta > 90^\circ$ , where all reported slip lengths have  $b < 20$  nm [8]. In particular, for dodecane against OTS-Pyrex ( $\theta = 28^\circ$ ), they reported a slip length  $b \sim 2$  nm, which is smaller than the value reported here ( $b \sim 15$  nm). All of our measurements are for liquids with contact angle  $\theta < 45^\circ$ ; therefore, our experiments are not necessarily inconsistent with a wettability-driven slip length at higher contact angles of  $\theta \sim 90^\circ$ . The difference in slip magnitude for dodecane may be due to one of the following: differences in silane chain length, differences in silane preparation, and/or our use of an environmental chamber, where filling is done under  $N_2$  gas. It has been shown in the past that differences in the silane deposition temperature can significantly alter the surface properties of  $n$ -alkylsilane coatings [18]. Also, our use of an environmental chamber minimizes contamination of the solid surfaces by atmospheric vapors.

In summary, we have used colloidal probe AFM to determine the slip behavior for the  $n$ -alkane and  $n$ -alcohol homologous series against a hydrophobic  $n$ -hexadecyltrichlorosilane-coated Si wafer. The slip lengths for these liquids obtained for separations  $h > 50$  nm were shear rate independent, where the hydrodynamic force quantitatively agreed with a theory by Vinogradova [7]. As the same colloidal probe and same Si wafer surface were used in studying all of these liquids, trends in the slip length can be attributed to changes in liquid properties. We find that the slip length  $b$  is predominantly a function of the bulk

viscosity  $\eta$ , where  $b=A\eta^x$  with  $A\sim 130\text{ nm}/(\text{Pa s})^x$  and  $x\sim 0.33$ . These results are similar to recent dewetting experiments [27] of polystyrene films on an  $n$ -alkylsilane-coated Si wafer, where the exponent  $x$  is a function of the grafted  $n$ -alkylsilane SAM chain length. A SAM chain length dependence of the microscale friction coefficient has been observed using friction force microscopy [31] and dynamic contact angle measurements [32]. A theoretical understanding of the interconnection between grafted layers, friction, and slip [33] will be required before these disparate experi-

mental observations can be interconnected. Future work with pure liquids on varying  $n$ -alkylsilane coated surfaces is needed to further understand the dependence of slip on viscosity.

The authors thank Dr. J.-H. Cho for assistance with the Igor Pro programming and Dr. N. V. Priezjev and Dr. J.-L. Barrat for discussions. This research was supported by the National Science Foundation under Grant No. DMR-0603144.

- 
- [1] E. Lauga, M. P. Brenner, and H. A. Stone, in *Springer Handbook in Experimental Fluid Mechanics*, edited by J. Foss, C. Tropea, and A. Yarin (Springer, New York, 2005), Chap. 15.
- [2] T. M. Squires and S. R. Quake, *Rev. Mod. Phys.* **77**, 977 (2005).
- [3] C. Cottin-Bizonne *et al.*, *Phys. Rev. Lett.* **94**, 056102 (2005).
- [4] C. D. F. Honig and W. A. Ducker, *Phys. Rev. Lett.* **98**, 028305 (2007).
- [5] C. I. Bouzigues, P. Tabeling, and L. Bocquet, *Phys. Rev. Lett.* **101**, 114503 (2008).
- [6] W. A. Ducker, T. J. Senden, and R. M. Pashley, *Nature (London)* **353**, 239 (1991).
- [7] O. I. Vinogradova, *Langmuir* **11**, 2213 (1995).
- [8] C. Cottin-Bizonne *et al.*, *Langmuir* **24**, 1165 (2008).
- [9] N. V. Priezjev and S. M. Troian, *Phys. Rev. Lett.* **92**, 018302 (2004).
- [10] A. Martini *et al.*, *Phys. Rev. Lett.* **100**, 206001 (2008).
- [11] C. Neto *et al.*, *Rep. Prog. Phys.* **68**, 2859 (2005).
- [12] V. S. J. Craig, C. Neto, and D. R. M. Williams, *Phys. Rev. Lett.* **87**, 054504 (2001).
- [13] Y. Zhu and S. Granick, *Phys. Rev. Lett.* **88**, 106102 (2002).
- [14] E. Lauga and M. P. Brenner, *Phys. Rev. E* **70**, 026311 (2004).
- [15] A. Steinberger *et al.*, *Phys. Rev. Lett.* **100**, 134501 (2008).
- [16] Z. Lin and S. Granick, *Langmuir* **19**, 7061 (2003).
- [17] O. I. Vinogradova *et al.*, *Rev. Sci. Instrum.* **72**, 2330 (2001).
- [18] J. B. Brzoska, I. Ben Azouz, and F. Rondelez, *Langmuir* **10**, 4367 (1994).
- [19] V. S. J. Craig and C. Neto, *Langmuir* **17**, 6018 (2001).
- [20] C. L. Yaws, *Handbook of Viscosity* (Gulf, Houston, 1995).
- [21] P. A. Thompson and M. O. Robbins, *Phys. Rev. A* **41**, 6830 (1990).
- [22] T. M. Galea and P. Attard, *Langmuir* **20**, 3477 (2004).
- [23] J.-L. Barrat and L. Bocquet, *Phys. Rev. Lett.* **82**, 4671 (1999).
- [24] D. M. Huang *et al.*, *Phys. Rev. Lett.* **101**, 226101 (2008).
- [25] A  $\sim 2$  nm zero of separation error changes the magnitude of  $b$  by  $\sim 1$  nm [see Eq. (3)].
- [26] L. Bocquet and J.-L. Barrat, *Soft Matter* **3**, 685 (2007).
- [27] R. Fetzer *et al.*, *Europhys. Lett.* **75**, 638 (2006).
- [28] W. W. Graessley, *Polymeric Liquids and Networks: Dynamics and Rheology* (Garland Science, London, 2008).
- [29] C. D. F. Honig and W. A. Ducker, *J. Phys. Chem. C* **111**, 16300 (2007); **112**, 17324 (2008).
- [30] P. G. de Gennes, *Rev. Mod. Phys.* **57**, 827 (1985).
- [31] X.-D. Xiao *et al.*, *Langmuir* **12**, 235 (1996).
- [32] M. Voué *et al.*, *Langmuir* **23**, 4695 (2007).
- [33] D. Long, A. Ajdari, and L. Leibler, *Langmuir* **12**, 1675 (1996); **12**, 5221 (1996).